The EMBO Journal (2010) 29, 606–618 | © 2010 European Molecular Biology Organization | All Rights Reserved 0261-4189/10
www.embojournal.org

THE EMBO JOURNAL

Antagonism of Beclin 1-dependent autophagy by BCL-2 at the endoplasmic reticulum requires NAF-1

Natasha C Chang, Mai Nguyen, Marc Germain[1] and Gordon C Shore*

Department of Biochemistry and Goodman Cancer Center, McGill University, Montreal, Quebec, Canada

In addition to mitochondria, BCL-2 is located at the endoplasmic reticulum (ER) where it is a constituent of several distinct complexes. Here, we identify the BCL-2-interacting protein at the ER, nutrient-deprivation autophagy factor-1 (NAF-1)—a bitopic integral membrane protein whose defective expression underlies the aetiology of the neurodegenerative disorder Wolfram syndrome 2 (WFS2). NAF-1 contains a two iron–two sulphur coordinating domain within its cytosolic region, which is necessary, but not sufficient for interaction with BCL-2. NAF-1 is displaced from BCL-2 by the ER-restricted BH3-only protein BIK and contributes to regulation of BIK-initiated autophagy, but not BIK-dependent activation of caspases. Similar to BCL-2, NAF-1 is found in association with the inositol 1,4,5-triphosphate receptor and is required for BCL-2-mediated depression of ER Ca^{2+} stores. During nutrient deprivation as a physiological stimulus of autophagy, BCL-2 is known to function through inhibition of the autophagy effector and tumour suppressor Beclin 1. NAF-1 is required in this pathway for BCL-2 at the ER to functionally antagonize Beclin 1-dependent autophagy. Thus, NAF-1 is a BCL-2-associated co-factor that targets BCL-2 for antagonism of the autophagy pathway at the ER.

The EMBO Journal (2010) **29,** 606–618. doi:10.1038/emboj.2009.369; Published online 10 December 2009
Subject Categories: membranes & transport; differentiation & death
Keywords: autophagy; BCL-2; Beclin 1; BIK; endoplasmic reticulum

Introduction

The BCL-2 family of proteins is responsible for regulating and executing the mitochondrial pathway of apoptosis. In addition, all three sub-groups of the family—the pro-survival members, the pro-apoptotic effectors BAX and BAK, and the pro-apoptotic BH3-only activators/sensitizers—are also found in association with the endoplasmic reticulum (ER) in which they regulate and modulate both mitochondrial-dependent and -independent apoptotic responses (Heath-Engel *et al*, 2008). More recently, several pro-survival members and BH3-only members have also been implicated in the regulation of macroautophagy (Levine *et al*, 2008), a quality control and cellular-survival mechanism that responds to conditions of nutrient and metabolic stress. In this pathway, pre-autophagosomal vesicles mature by engulfing organelles and cytoplasmic complexes, encapsulating these contents within a double membrane vesicle, which subsequently fuses with lysosomes. The resulting degradation of autophagosomal contents regenerates macromolecule precursors that otherwise could not be generated if their metabolic biosynthesis was repressed (Yorimitsu and Klionsky, 2005).

Recent studies suggest that pre-autophagosomal vesicles are generated at an ER-associated location, the omegasome, which represents a specialized, phosphatidylinositol 3-phosphate (PI(3)P)-enriched ER membrane platform for assembly of a phagosomal initiation complex (Axe *et al*, 2008). This platform seems to be created through recruitment to the ER of vesicles-containing Vps34, a class III phosphatidylinositol 3-kinase (PI3K) that associates with Beclin 1 and other accessory proteins to generate a functional PI3K complex (Kihara *et al*, 2001), thus resulting in enrichment of PI(3)P at this ER-associated site (Axe *et al*, 2008). The exact topography of the assembly of the PI3K complex at this site, however, remains to be determined. Beclin 1 is a haploinsufficient tumour suppressor and an important effector of autophagy, whose antagonism can be achieved by BCL-2 that is located at the ER (Liang *et al*, 1999; Pattingre *et al*, 2005). Beclin 1 contains a BH3 domain that contributes to its interaction with BCL-2, but the avidity of this interaction is quite weak compared with BH3 domains present in the BH3-only proteins typically associated with apoptosis regulation (Feng *et al*, 2007; Oberstein *et al*, 2007). Moreover, BH3-containing Beclin 1 does not seem to antagonize the anti-apoptotic function of BCL-2 at either the ER or mitochondria (Ciechomska *et al*, 2009). Thus, canonical BH3-only proteins such as BAD have been shown to displace Beclin 1 from BCL-2 (Maiuri *et al*, 2007), leading to the proposal that a signalling cascade analogous to the release of BCL-2 antagonism by BH3-only proteins in the apoptosis pathway also extends to autophagy (Levine *et al*, 2008). In addition, phosphorylation of the Beclin 1 BH3 region by the death-associated protein kinase (DAPk) pathway (Zalckvar *et al*, 2009) or of BCL-2 in the c-Jun N-terminal protein kinase (JNK) pathway (Wei *et al*, 2008) has been linked to disruption of Beclin 1/BCL-2 or BCL-XL interactions. In addition to BCL-2 interactions with Beclin 1 at the ER, BCL-2 can also interact with BAX (White *et al*, 2005), with the BAP31 complex (Breckenridge *et al*, 2002), and with the calcium-conducting inositol 1,4,5-triphosphate (IP3) receptor (Chen *et al*, 2004) at this location. In view of these multiple BCL-2-associated pathways at the ER and the relatively weak bind-

*Corresponding author. Department of Biochemistry, McGill University, McIntyre Medical Sciences Building, Room 906B, 3655 Promenade Sir William Osler, Montreal, Quebec, Canada H3G 1Y6.
Tel.: +1 514 398 7282; Fax: +1 514 398 7384;
E-mail: gordon.shore@mcgill.ca
[1]Present address: Department of Cellular and Molecular Medicine, University of Ottawa, Ottawa, Ontario, Canada K1H 8M5

Received: 12 May 2009; accepted: 13 November 2009; published online: 10 December 2009

ing between BCL-2 and Beclin 1, mechanisms presumably exist to ensure adequate partitioning of ER BCL-2 to the autophagy pathway at this organelle. Emerging genetic (Lam *et al*, 2008) and biochemical evidence (Criollo *et al*, 2007; Vicencio *et al*, 2009), for example, have identified the IP3 receptor complex as important in Beclin 1-mediated autophagy, by providing a potential scaffold for regulating BCL-2 and Beclin 1 interactions and/or for modulating autophagy in response to BCL-2-regulated stores of ER Ca^{2+}.

Here, we have identified a novel protein-binding partner of BCL-2 at the ER, nutrient-deprivation autophagy factor-1 (NAF-1). The interaction between NAF-1 and BCL-2 is independent of a BH3 domain, but rather depends on the two iron–two sulphur (2Fe-2S) coordinating CDGSH domain of NAF-1. Whereas NAF-1 is not required for BCL-2 to interact with BH3-only BIK, NAF-1 contributes to the interaction of BCL-2 with Beclin 1 and is required for BCL-2 to functionally antagonize Beclin 1-mediated cellular autophagy in response to nutrient deprivation of H1299 epithelial cells in culture. Of note, NAF-1—similar to BCL-2 and Beclin 1—is a component of the IP3 receptor complex and is required for BCL-2 to depress ER Ca^{2+} stores. ER-restricted NAF-1, therefore, is a BCL-2-associated co-factor that helps target BCL-2 antagonism to the Beclin 1-dependent autophagy pathway at the ER.

Results

NAF-1 interacts with BCL-2 at the ER and is displaced by BIK

Immunoblotting of ER proteins derived from the human carcinoma cell line H1299 and resolved by non-denaturing 2D gel electrophoresis established that BCL-2 at the ER migrates both as a monomer and as part of larger complexes (data not shown). Part of the BCL-2 population co-migrated with its binding partner IP3 receptor (Chen *et al*, 2004; Oakes *et al*, 2005), as well as with other complexes devoid of IP3 receptor. To investigate the composition of BCL-2 complexes, light membrane (LM) enriched in ER was isolated from H1299 cells stably expressing ER-targeted HA-BCL-2b5, in which the BCL-2 transmembrane (TM) segment was replaced with that of ER-selective cytochrome b5 (Zhu *et al*, 1996; Germain *et al*, 2005). Chemical cross-linking was performed with the homo-bifunctional Cys-specific agent, bis-maleimidohexane (BMH). Analysis of cross-linked complexes by SDS–PAGE and immunoblotting with anti-BCL-2 antibody confirmed that BCL-2 at the ER is present in complexes of heterogeneous size (Figure 1A). As a filter for specificity, we focused on those complexes in which BCL-2 can be displaced from the complex by BIK, a BH3-only protein that localizes predominantly to the ER and binds strongly to BCL-2 (Boyd *et al*, 1995; Mathai *et al*, 2002). BIK was delivered using an adenovirus expression system (either as Ad-BIK or Ad-BIKb5). We focused on one of these BCL-2-displaced complexes (denoted with a bold arrow in Figure 1A) and identified the cross-linked BCL-2-binding partner (Supplementary Figure 1), which we designated as NAF-1.

The NAF-1 sequence (Figure 1B; 135 aa; 15 278 daltons), which is widely expressed, was originally disclosed in a former analysis of the subcellular localization of novel proteins identified by large-scale human cDNA sequencing (Simpson *et al*, 2000). A BLAST search of the NAF-1 amino-acid sequence revealed that NAF-1 is evolutionarily conserved, with orthologues of unknown function in species ranging from *C. elegans* to human (Supplementary Figure 2). Of note, the NAF-1 sequence does not seem to contain a canonical BH3 domain. Displacement of the NAF-1 interaction with BCL-2 by BIK, therefore, is unlikely to be the result of simple competitive binding for the BH3-binding groove of BCL-2. Hydrophobicity analysis predicts the presence of a single TM segment (aa 41–60); all four Cys residues that are potentially available for cross-linking with BMH are C-terminal of this segment and the C-terminus ends in KKEV, which corresponds to the canonical cytosolic-disposed ER retrieval motif for integral ER proteins, KKxx (where x is any amino acid; Jackson *et al*, 1990). As the lone Cys residue in BCL-2 that is available for cross-linking resides in the BCL-2 cytosolic domain, this means that NAF-1 is predicted to be oriented in the ER membrane as shown in Figure 1C and consistent with the predicted cytosolic disposition of the KKEV C-terminus.

Interestingly, another recent report has established that NAF-1 is a key protein involved in the Wolfram syndrome 2 (WFS2) neurodegenerative disorder. A single missense mutation was identified in the gene encoding NAF-1, *wfs2*, resulting in abnormal splicing of the messenger RNA and introduction of a premature stop codon, which truncates 75% of the protein (Amr *et al*, 2007). No attribution to the function of either the wild-type or mutant NAF-1 protein was reported. In addition, NAF-1 was also recently identified as part of a three-member family of proteins, which contain a unique CDGSH iron/sulphur-binding domain (Figure 1B and C). Unlike its other two family members, which localize to the mitochondria, NAF-1 is distinct in that it localizes to the ER (Wiley *et al*, 2007a; see also below). The founding member of this family, mitoNEET at the mitochondria, has been shown to bind a 2Fe-2S cluster, which is coordinated by three Cys and one His residues within the CDGSH domain (Wiley *et al*, 2007b). Neither the function of this domain nor of this family of proteins, however, has been determined. Recent targeted disruption of the *wfs2* gene in mice, however, resulted in an early onset of ageing and mortality (Chen *et al*, 2009).

The initial observation of NAF-1 as an interacting partner of BCL-2b5 was the result of chemical cross-linking. We confirmed this interaction by precipitation of the cross-linked BCL-2 product with anti-NAF-1 antibody and blotting with anti-BCL-2 antibody (Figure 1D). We also confirmed that BH3-only BIK displaces NAF-1 from BCL-2b5. Purified LM from H1299 HA-BCL-2b5 cells that had been either mock infected or infected with Ad-BIK were subjected to cross-linking and subsequent immunoprecipitation with anti-NAF-1 antibody. Significantly less NAF-1/BCL-2 dimer was precipitated in the presence of BIK expression (Figure 1E). Thus, although NAF-1 likely interacts with BCL-2 through a BH3-independent mechanism, it can still be displaced from BCL-2 by a BH3-only protein. This could be the result of a conformational change in BCL-2 induced by the BH3-only binding partner (Dlugosz *et al*, 2006). Alternatively, it could arise because BIK disrupts a larger complex that contributes to NAF-1/BCL-2 interactions.

Using SK-Mel5 cells, endogenous NAF-1 was shown to interact with endogenous wild-type BCL-2 by co-immunoprecipitation (Figure 2A). Similar results were obtained for BCL-XL (Supplementary Figure 3). As expected (and in agreement with Wiley *et al*, 2007a), immunofluorescence

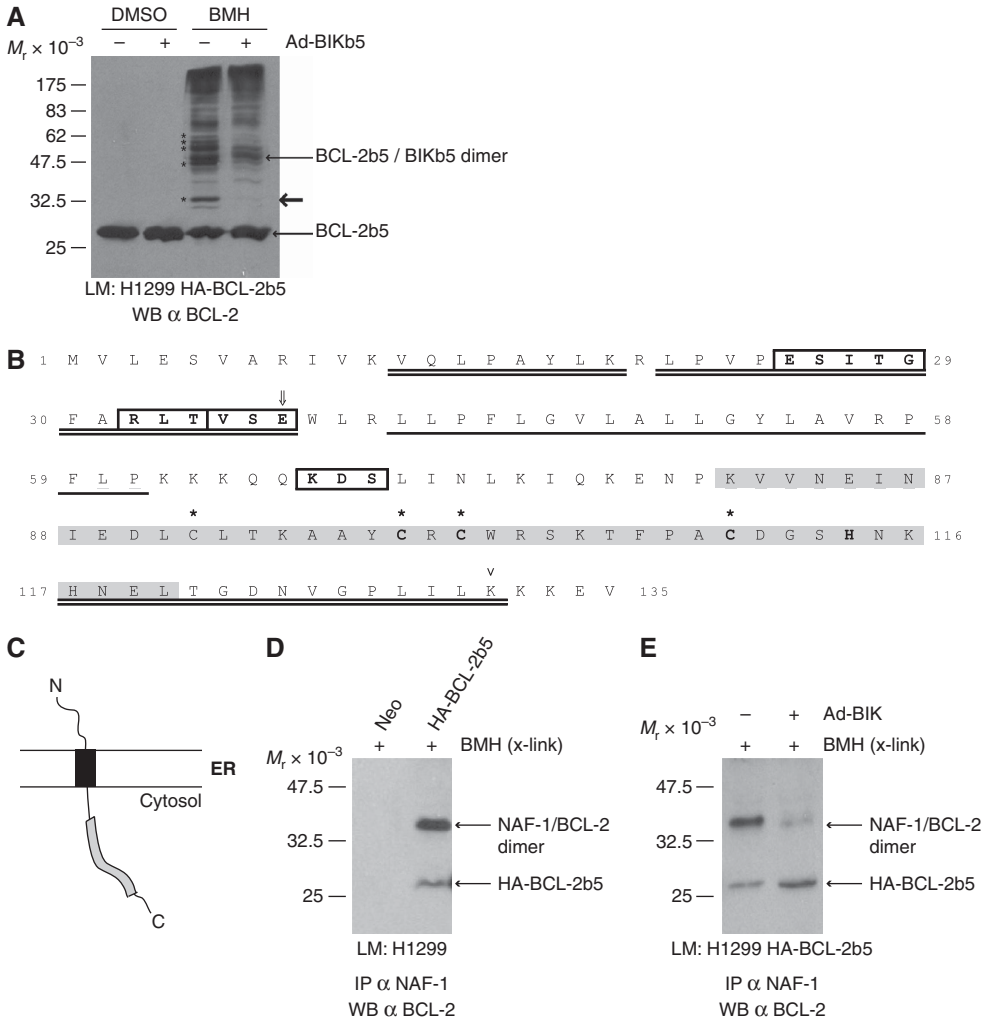

Figure 1 Identification of a novel BCL-2-interacting partner, NAF-1, at the ER. (**A**) BH3-only BIK displaces a subset of BCL-2 complexes at the ER. Purified LM from H1299 HA-BCL-2b5 cells either mock infected or infected with Ad-BIKb5 was subjected to cross-linking with BMH and visualized by immunoblot. Asterisks (*) denote BCL-2 cross-linked products, which are displaced by BIK. Bold arrow denotes region containing cross-linked NAF-1/BCL-2. (**B**) Amino-acid sequence of NAF-1. Peptide sequences identified by mass spectrometry are indicated by a double underline. The TM domain is indicated by a bold single underline. Cys residues in the cytosolic domain are denoted with asterisks (*). The CDGSH domain is highlighted in grey, and the predicted 2Fe-2S coordinating Cys-3-His-1 aa are marked in bold. A downwards arrow head (∨) represents the site in which a Flag epitope was inserted. A double-lined arrow (⇓) indicates the Glu residue that when mutated (E37Q) causes WFS2. Predicted phosphorylation sites found using the PhosphoMotif Finder from the Human Protein Reference Database (HPRD) are indicated in bold within a box; β-adrenergic receptor kinase substrate motif (aa 25–29), PKA and PKC kinase substrate motifs (aa 32–34 and 67–69), and casein kinase II substrate motif (aa 34–37). (**C**) Deduced membrane topology of NAF-1. Grey rectangle indicates CDGSH domain. (**D**) Endogenous NAF-1 cross-links with BCL-2 at the ER. LM purified from H1299 neo and HA-BCL-2b5 cells were subjected to cross-linking by BMH and immunoprecipitation with anti-NAF-1 antibody. Precipitates were analysed by immunoblot with anti-BCL-2. (**E**) NAF-1 is displaced from BCL-2 by BH3-only BIK. H1299 HA-BCL-2b5 cells were either mock infected or infected with Ad-BIK. Purified LM was treated as in (**D**).

analysis indicated that endogenous NAF-1 distributed primarily to the ER in H1299 cells (Figure 2B). We also confirmed that the primary translation product of NAF-1-Flag in rabbit reticulocyte lysate efficiently targeted and inserted into dog pancreas microsomes *in vitro* (Wang *et al*, 2008) in which it acquired resistance to extraction by $NaCO_3$, pH 11.5 (diagnostic of membrane integration), but not into purified heart mitochondria (McBride *et al*, 1992; Supplementary Figure 4). In contrast, HA-BAK targeted and inserted into both ER microsomes and mitochondria. The findings that NAF-1 resides primarily at the ER (Wiley *et al*, 2007a; this study) contrasts with the conclusions of Chen *et al* (2009), who suggest a primarily mitochondrial location. This was based on ectopic analysis of over-expressed GFP-fusion protein and cell fractionation that did not include an ER marker.

An adenovirus vector was created that expresses full-length NAF-1 containing a Flag-tag just upstream of the KKEV ER retention signal (Figure 1B), and we verified that NAF-1-Flag interacted with BCL-2b5 by co-immunoprecipitation (Figure 2C). As a signature site in NAF-1 is the 39 amino-acid-long CDGSH domain, we mutated the corresponding critical three Cys and the His residues, which were shown to be important for binding the 2Fe-2S cluster in mitoNEET (Figure 1B; Wiley *et al*, 2007b). The three Cys residues were converted to Ser and the His residue was converted to Gln (C99S C101S C110S H114Q), and this modified protein was

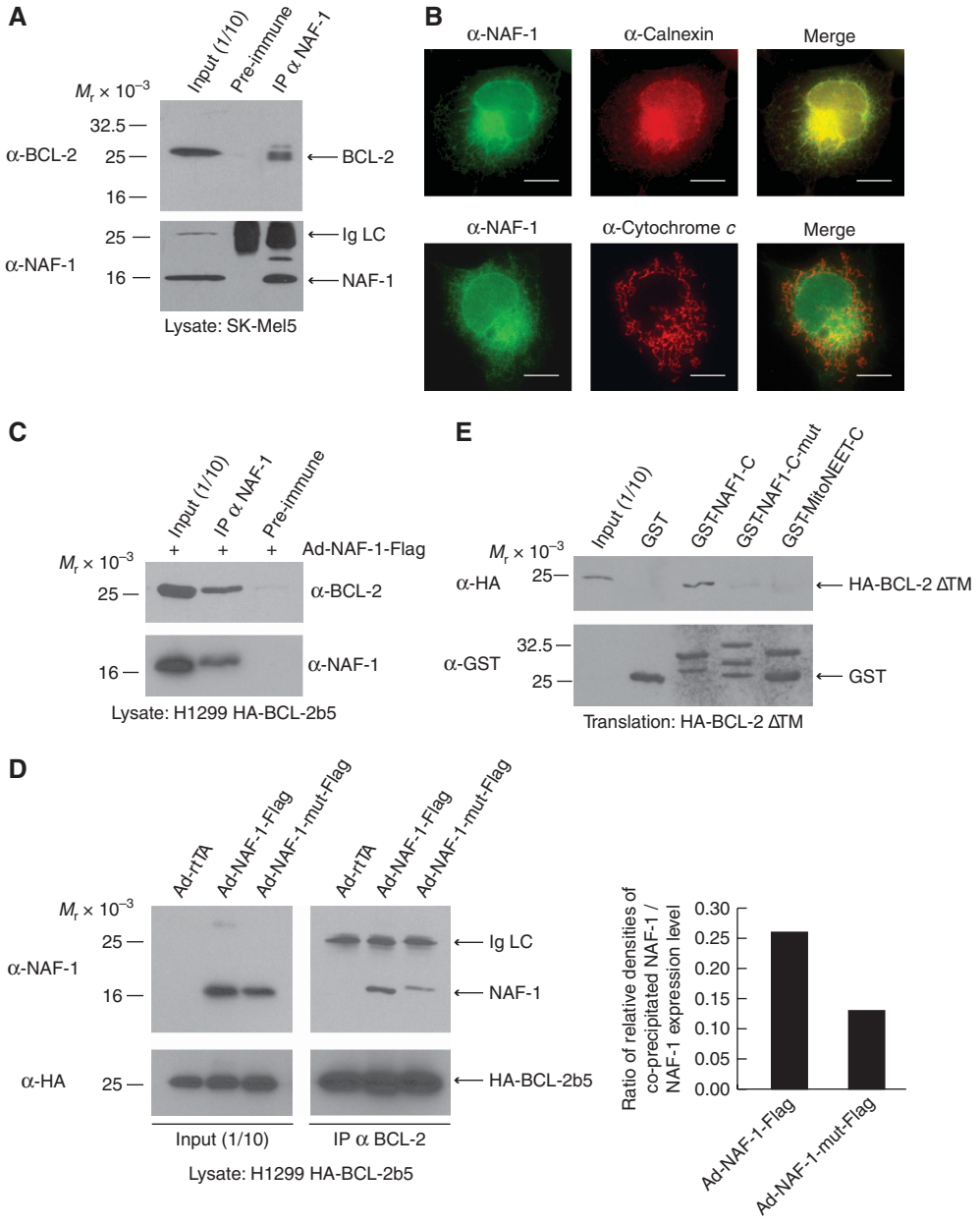

Figure 2 The NAF-1/BCL-2 interaction. (**A**) Co-immunoprecipitation of endogenous NAF-1 and BCL-2. Lysates from SK-Mel5 cells were collected and immunoprecipitation was performed with anti-NAF-1 antibody. The precipitate was subjected to immunoblotting with anti-BCL-2 and anti-NAF-1. (**B**) H1299 cells were fixed and double stained with anti-NAF-1 and anti-Calnexin or anti-Cytochrome *c* antibodies. Scale bar represents 10 μm. (**C**) Co-immunoprecipitation of NAF-1-Flag and HA-BCL-2b5. Lysates from H1299 HA-BCL-2b5 cells infected with Ad-NAF-1-Flag were collected and treated as in (**A**). (**D**) Mutations in the CDGSH iron-binding domain of NAF-1 interfere with NAF-1 binding to BCL-2. H1299 HA-BCL-2b5 cells were infected with either Ad-rtTA, Ad-NAF-1-Flag, or Ad-NAF-1-mut-Flag (C99S C101S C110S H114Q). Lysates were treated as in (**A**). Densitometric analysis was performed using Scion Image software to quantify expression and co-precipitated levels of NAF-1-Flag and NAF-1-mut-Flag. Graph depicts the ratio of co-precipitated protein to expression level. (**E**) A functional CDGSH iron-binding domain is necessary, but not sufficient for the interaction between the cytosolic domains of NAF-1 and BCL-2. HA-BCL-2 ΔTM was *in vitro* translated in rabbit reticulocyte lysate and equivalent aliquots were added to each GST pull-down reaction. GST-fusion proteins used were GST alone, GST-NAF1-C, GST-NAF1-C-mut (C99S C101S C110S H114Q), and GST-MitoNEET-C. The proteins were detected using anti-HA and anti-GST.

designated NAF-1-mut. Lysates were collected from H1299 HA-BCL-2b5 cells infected with adenovirus-expressing NAF-1-Flag, NAF-1-mut-Flag, or rtTA protein (control), and immunoprecipitation was performed with anti-BCL-2 antibody. Significantly less NAF-1-mut co-precipitated with BCL-2 compared with wild-type NAF-1, whereas similar amounts of BCL-2 were precipitated (Figure 2D). The CDGSH domain, therefore, contributes to the interaction between NAF-1 and BCL-2.

GST-fusion proteins were created, which contain the cytosolic domains of NAF-1 (GST-NAF1-C), of the Cys-3-His-1 NAF-1 mutant (GST-NAF1-C-mut), or of mitoNEET (GST-MitoNEET-C). Of note, the GST-NAF1-C and GST-MitoNEET-C proteins were rust coloured after purification on glutathione beads signifying their ability to bind iron as earlier documented (Wiley *et al*, 2007a). In contrast, GST-NAF1-C-mut was devoid of rust colour. GST and the GST-fusion proteins were conjugated to glutathione beads and incubated with *in vitro*

translated HA-BCL-2 ΔTM (cytosolic BCL-2 lacking the TM domain) in reticulocyte lysate. BCL-2 ΔTM was pulled down by GST-NAF1-C, confirming that the two proteins interact through their respective cytoplasmic domains (Figure 2E). In accordance with the co-immunoprecipitation data, GST-NAF1-C-mut did not pull down BCL-2 ΔTM, reaffirming the importance of the CDGSH domain for this interaction. Interestingly, cytosolic mitoNEET, which contains a functional CDGSH domain, did not pull down BCL-2 ΔTM, signifying that while a functional CDGSH domain is necessary, it is likely not sufficient for the interaction between NAF-1 and BCL-2. Other elements within the protein sequence of NAF-1 besides a functional CDGSH domain, therefore, likely contribute to the interaction of NAF-1 with BCL-2.

NAF-1 contributes to regulation of BIK-initiated autophagy, but not BIK-initiated activation of caspases

Lentivirus encoding small hairpin RNA (shRNA) targeted against NAF-1 mRNA was used to knock down NAF-1 expression in H1299 neo and H1299 BCL-2b5 cells (Figure 3A). Knockdown of NAF-1 had no effect on the ability of Ad-BIK to induce the activation of caspase-3, as determined by immunoblot of the catalytic subunit cleaved from procaspase-3 (Figure 3A, lanes 5 and 6) or by assay of DEVDase activity (Figure 3B), nor did knockdown influence the ability of BCL-2 to antagonize these outcomes (Figure 3A, lanes 7 and 8; B). The pan caspase inhibitor zVAD-fmk strongly inhibited induction of caspase-3 by BIK (Figure 3A and B), and this extended for many hours (data not shown). Prolonged expression of BIK in cells in which apoptosis is inhibited by zVAD-fmk, however, has been shown to lead to caspase-independent cell death with autophagic features (Rashmi *et al*, 2008). Thus, cell lysates were analysed by immunoblot (Swerdlow *et al*, 2008) for conversion of the cytoplasmic form of microtubule-associated protein 1 light chain 3 (LC3 I form) to LC3 II, which is widely used to assay autophagosome accumulation (Mizushima and Yoshimori, 2007; Figure 3C). In the absence of caspase activation (zVAD-fmk treatment), BIK expression over 30 and 48 h caused a progressive loss of LC3 I (Figure 3C, compare lanes 1, 5, and 9). The most dramatic consequence of

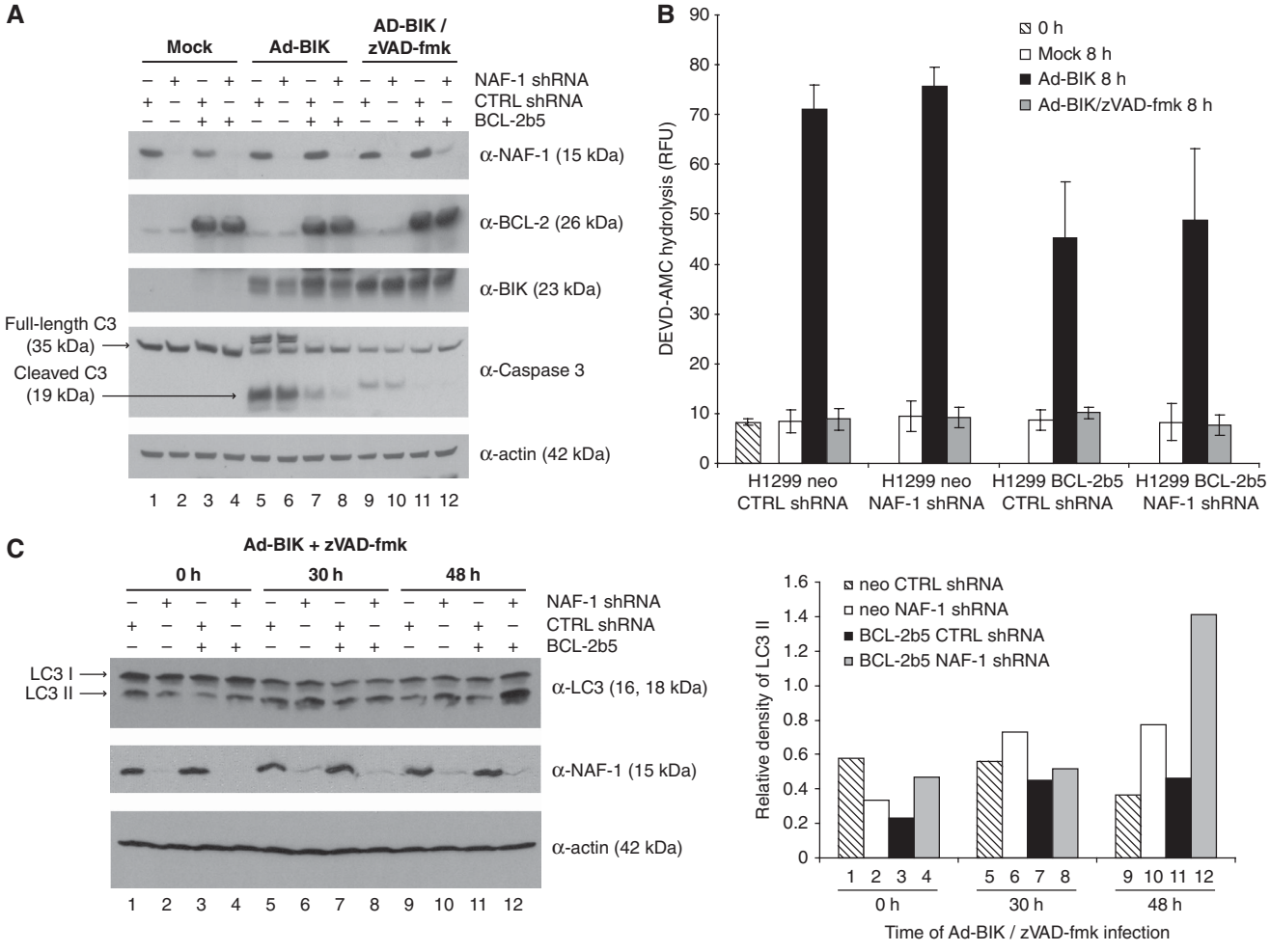

Figure 3 NAF-1 does not affect BIK-initiated apoptosis, but influences BIK-induced autophagy in the absence of caspase activation. (**A**) H1299 neo and HA-BCL-2b5 cells treated with control (CTRL) or NAF-1 shRNA were either mock infected or infected with Ad-BIK in the absence or presence of 50 μM zVAD-fmk. Cell lysates were analysed by immunoblot. (**B**) Caspase activity was measured using the fluorescent substrate DEVD-AMC. The results represent the average ± s.d. of three independent experiments. (**C**) Prolonged BIK expression and caspase inhibition induces autophagy, which is enhanced by knockdown of NAF-1. H1299 neo and HA-BCL-2b5 cells treated with CTRL or NAF-1 shRNA were infected with Ad-BIK in the presence of zVAD-fmk for the indicated periods of time. Cell lysates were analysed by immunoblot. Levels of LC3 II were normalized to actin levels by densitometry analysis. Graph depicts normalized LC3 II levels of each lane.

NAF-1 shRNA knockdown occurred in the presence of BCL-2b5, in which BIK induced a significant increase in the ratio of LC3 II to LC3 I at 48 h (Figure 3C, lane 12) compared with control (CTRL) shRNA (Figure 3C, lane 11). Consistent with the physical association between BCL-2 and NAF-1, these results suggest a potential functional relationship between these proteins in the regulation of autophagy. However, the autophagic response to BIK was quite sluggish (30–48 h versus 8 h for apoptosis induction); moreover, it required co-application with zVAD-fmk to manifest, and as yet has not been implicated in a physiological pathway of autophagy. Thus, we explored the functional relationship between BCL-2 and NAF-1 in autophagy during the rapid and physiological response to nutrient deprivation. Although nutrient deprivation does not induce BIK (data not shown), the results with BIK clearly show that the NAF-1/BCL-2 complex could be a target of a BH3-only protein.

Contribution of NAF-1 to BCL-2-mediated antagonism of Beclin 1-dependent autophagy during nutrient deprivation

The autophagic process is dynamic in nature and LC3 II is degraded after fusion of autophagosomes with lysosomes. Hence, to permit the use of comparative LC3 II levels as a measure of autophagic response, an inhibitor of vacuolar type (H+)-ATPase, bafilomycin A1 (Baf A1), was used to prevent the fusion of autophagosomes with lysosomes (Mizushima and Yoshimori, 2007). H1299 cells that had been treated with CTRL or NAF-1 shRNA were starved in Earle's balanced salt solution (EBSS) for 4 h in the presence of DMSO (vehicle) or Baf A1 and examined by immunoblot. In the presence of inhibitor, there was increased accumulation of LC3 II in NAF-1 shRNA-treated starved cells compared with control shRNA (Figure 4A, top panel, lanes 5 and 6). This suggests that NAF-1 contributes to a restraint on starvation-induced autophagy. To rule out the possibility that nutrient deprivation in the absence of NAF-1 induces the apoptotic pathway, we examined the cells for procaspase-3 processing and detected only full-length procaspase-3 in both CTRL and NAF-1 shRNA-treated cells (Figure 4A). Again, this signifies a function for NAF-1 in autophagy as opposed to apoptosis.

Fluorescent GFP-LC3 is used extensively to measure autophagy as it displays a uniform cytoplasmic distribution under normal conditions and fluorescently labels autophagosomes as punctate structures within the cytoplasm under autophagy-inducing conditions (Mizushima *et al*, 2004). To avoid protein aggregation problems commonly observed in cells transiently over-expressing GFP-LC3, we generated H1299 cell lines that stably express GFP-LC3 and have confirmed that these cells are autophagy competent. H1299 GFP-LC3 cells were transfected with NAF-1 siRNA or control (LUC) siRNA and either maintained in normal media (untreated) or starved for 4 h in EBSS (Figure 4B and C). Untreated cells transfected with LUC siRNA displayed diffuse GFP-LC3 staining, whereas starved cells displayed punctate GFP-LC3 resembling typical autophagy induction. NAF-1 knockdown had no effect on autophagy in nutrient-replete cells. Interestingly, however, starved cells with reduced NAF-1 expression (NAF-1 siRNA) exhibited differences compared with the starved LUC control, which was manifested as two types of starvation phenotypes (Figure 4B). A total of 25% of cells lacking NAF-1 displayed a morphology after starvation similar to that of starved control cells. The majority of starved cells lacking NAF-1 (75%), however, displayed a phenotype that included larger fluorescent GFP-LC3 puncta as well as the distribution of GFP-LC3 in membrane blebs or filopodia at the cell periphery. Of note, similar membrane blebbing and accumulation of large GFP-LC3-positive autophagic vesicles has been reported as a phenotype associated with cell death mediated by DAPk family members (Inbal *et al*, 2002).

The Beclin 1 dependency of autophagy mediated by NAF-1 knockdown in starved cells was investigated in H1299 GFP-LC3 cells that were transfected with siRNA directed against either LUC, Beclin 1, NAF-1, or both Beclin 1 and NAF-1 in combination. Autophagy levels for each sample were quantified as the percentage of GFP-LC3-expressing cells that displayed punctate GFP-LC3. As expected, induction of GFP-LC3 aggregation on starvation for 4 h was dependent on Beclin 1 (Figure 4C; Beclin 1 siRNA). The enhanced autophagy after NAF-1 knockdown in starved cells was also negated by knockdown of Beclin 1 expression (Figure 4C; Beclin 1 + NAF-1 siRNA), indicating that NAF-1 operates within and upstream of Beclin 1 in the canonical Beclin 1-mediated autophagy pathway. In contrast, ectopic over-expression of NAF-1 provided no additional restraint over endogenous levels of NAF-1 on autophagy activity in this pathway (data not shown). However, as NAF-1 is a BCL-2-interacting protein, the autophagic restraint conferred by NAF-1 may be coupled to BCL-2.

BCL-2 residing at the ER has been reported to bind to the essential autophagy protein Beclin 1 and to inhibit Beclin 1-dependent starvation-induced autophagy (Pattingre *et al*, 2005). As shown in Figure 5A, NAF-1 knockdown significantly reduced the interaction between BCL-2b5 and Beclin 1 in H1299 HA-BCL-2b5 cells transfected with Flag-Beclin 1, as judged by co-immunoprecipitation. Furthermore, clear evidence for a contribution of NAF-1 to the functional antagonism of Beclin 1-mediated autophagy by BCL-2 was obtained. H1299 cell lines stably expressing GFP-LC3 and either neo or BCL-2b5 were generated and transfected with either LUC siRNA or NAF-1 siRNA, with or without subsequent starvation. Similar to that observed in Figure 4B and C, knockdown of NAF-1 had no effect on GFP-LC3 distribution in the absence of cell starvation for either neo or BCL-2b5 cells (data not shown). The number of cells exhibiting punctate GFP-LC3 after starvation was significantly reduced in BCL-2b5 cells treated with control LUC siRNA, compared with neo cells (Figure 5B). Knockdown of NAF-1, however, prevented BCL-2b5 from antagonizing starvation-induced autophagy as judged by the accumulation of GFP-LC3 puncta (Figure 5B), showing that BCL-2 inhibition of autophagy requires NAF-1. These results were confirmed by electron microscopy (Figure 5C–E), as judged by quantification of autophagosome vacuoles. H1299 neo LUC siRNA cells in the absence of starvation displayed virtually no autophagosomal structures (Figure 5Ca), whereas their starved counterpart (Figure 5Cb) exhibited autophagosomal structures typical of autophagy induction. Induction of these autophagosomes was inhibited by BCL-2b5 (Figure 5Cd). The majority of the starved H1299 neo cells lacking NAF-1 (Figure 5Cc) exhibited more autophagosomes per cell compared with LUC siRNA starved cells (Figure 5Cb and E), thus portraying an enhanced autophagy response. Importantly, elevated autophagosomes in starved H1299 BCL-2b5 cells lacking NAF-1 was observed

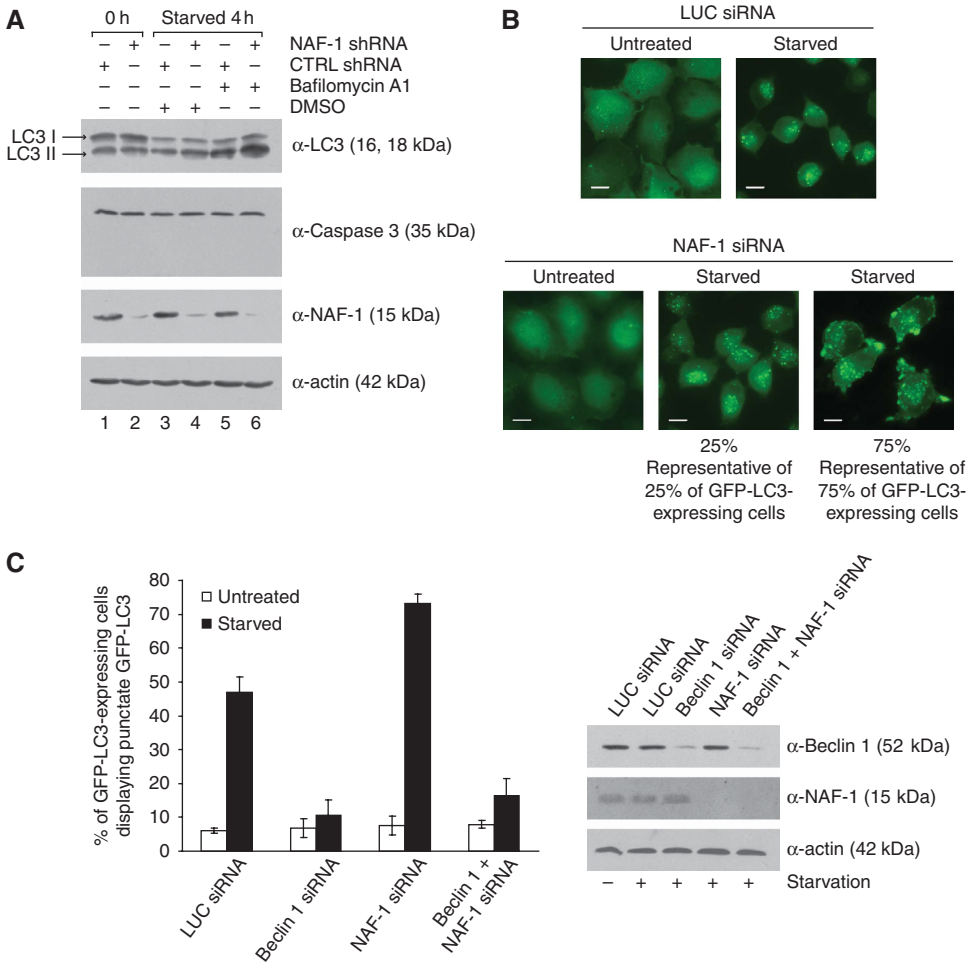

Figure 4 NAF-1 knockdown results in increased incidence and intensity of starvation-induced Beclin 1-dependent autophagy. (**A**) Effect of NAF-1 knockdown on starvation-induced autophagy. H1299 cells infected with CTRL or NAF-1 shRNA were starved for 4 h in EBSS with DMSO (vehicle) or Baf A1 (100 nM). Cell lysates were analysed by immunoblot. (**B**) Representative images of GFP-LC3 staining in H1299 GFP-LC3 cells transfected with LUC or NAF-1 siRNA, untreated and starved. Scale bar represents 10 μm. (**C**) Quantification of autophagy is expressed as the percentage of GFP-LC3-expressing cells displaying punctate GFP-LC3. A minimum of 100 cells per sample were counted; results represent the average ± s.d. of three independent experiments. Cell lysates were analysed by immunoblot.

(Figure 5Ce and E), as was the number of cells with elevated autophagosomes (Figure 5D), again indicating that inhibition of starvation-induced autophagy by BCL-2b5 requires NAF-1. The incidence of autophagy was determined by measuring the number of cells containing autophagic vacuoles as a percentage of total cells counted (Figure 5D) and by counting the number of autophagosomes per cell for each sample (Figure 5E), which closely mirrored the data obtained with fluorescent GFP-LC3 (Figures 4C and 5B).

Of note, we have extensively reviewed our electron micrograph analyses of control and NAF-1 knockdown cells, with and without nutrient starvation, and did not observe any obvious effect of NAF-1 knockdown on either mitochondrial morphology (including fragmentation) or proximity to ER. Although this does not rule out an effect on mitochondrial or ER-mitochondrial functions, if such an effect is present, it is not manifested by overt morphological changes in the time frame (4 h) and experimental system used here.

Finally, as BCL-2b5 effectively blocks autophagy in response to nutrient deprivation and this is dependent on its binding partner NAF-1, we confirmed that this physical association between the two proteins was retained after starvation. As shown in Supplementary Figure 5, equivalent co-immunoprecipitation of endogenous BCL-2 and endogenous NAF-1 was observed in SK-Mel5 cells with and without nutrient starvation for 4 h.

Physical and functional association of NAF-1 with the IP3 receptor

An important target of BCL-2 at the ER is the IP3 receptor (Chen *et al*, 2004; Oakes *et al*, 2005), the main channel in the ER for efflux of ER Ca^{2+}. Similar to the interaction of BCL-2 with NAF-1, the interaction of BCL-2 with the IP3 receptor does not involve the BCL-2 BH3-binding groove (Rong *et al*, 2009). In addition, both genetic (Lam *et al*, 2008) and biochemical (Criollo *et al*, 2007; Vicencio *et al*, 2009) evidence has implicated the IP3 receptor in the regulation of autophagy. A hallmark consequence of elevated BCL-2 at the ER in epithelial cells is a depression of the level of ER luminal stores of mobile Ca^{2+} (Pinton and Rizzuto, 2006). ER Ca^{2+} can be rapidly purged through the IP3 receptor by blocking the SERCA ATPase, which is responsible for Ca^{2+} uptake into the organelle. Thus, treatment of cells with the SERCA ATPase inhibitor thapsigargin (TG) results in an

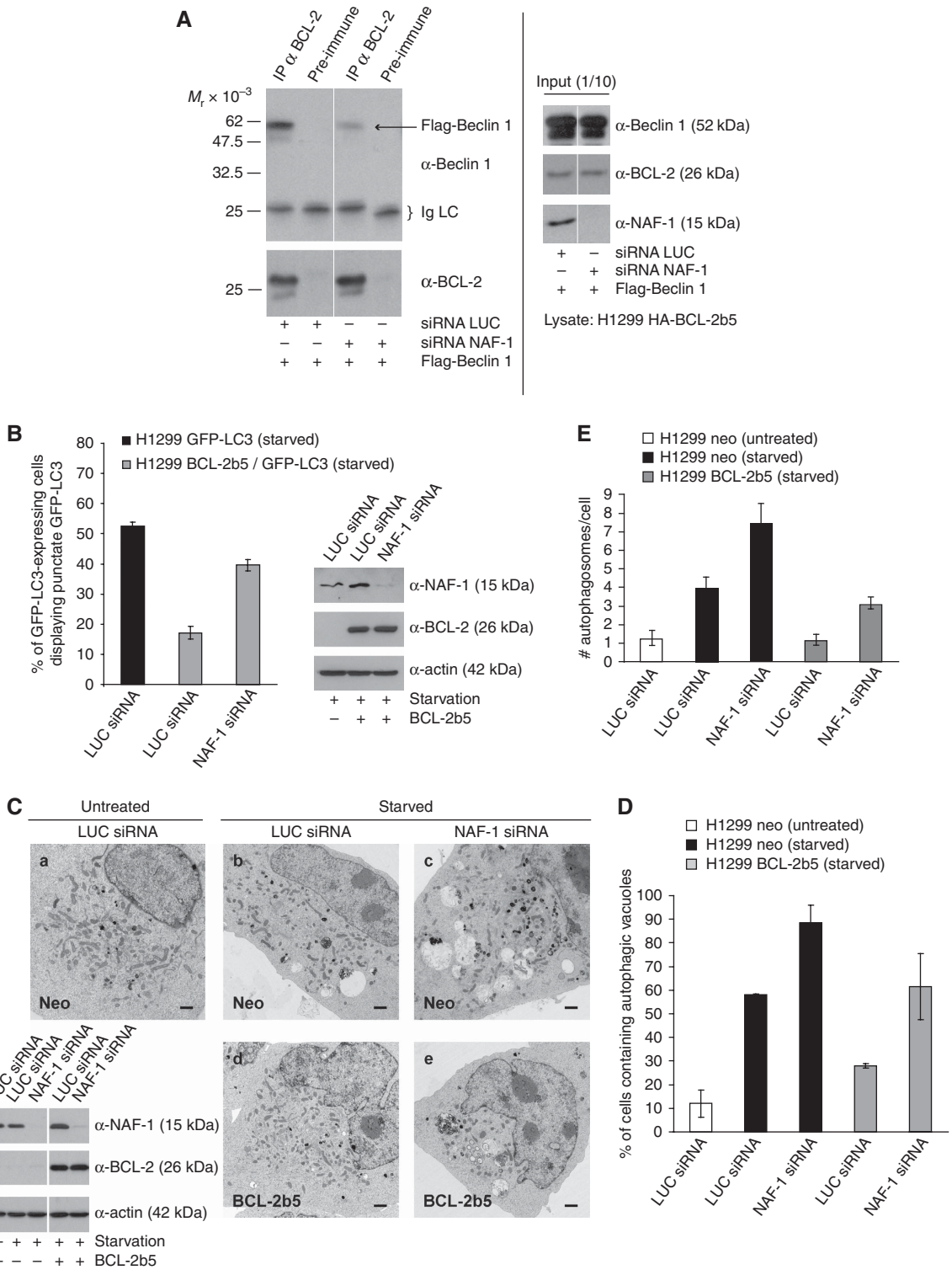

Figure 5 BCL-2 inhibition of Beclin 1-dependent autophagy requires NAF-1. (**A**) NAF-1 contributes to the interaction between BCL-2 and Beclin 1. H1299 HA-BCL-2b5 cells were transfected with Flag-Beclin 1 and either LUC or NAF-1 siRNA. Cells were lysed and subjected to immunoprecipitation with anti-BCL-2 antibody. Precipitates were subjected to analysis by immunoblot using anti-Beclin 1 and anti-BCL-2. All lanes are derived from the same gel and of the same exposure. Thin white lines indicate where lanes have been removed. (**B**) Loss of NAF-1 prevents BCL-2b5 from antagonizing starvation-induced autophagy. H1299 GFP-LC3 and BCL-2b5/GFP-LC3 cells were transfected with either LUC or NAF-1 siRNA and starved for 4 h. Cells were analysed as in Figure 4C. (**C**) Representative electron micrographs of H1299 neo and HA-BCL-2b5 cells treated with either LUC or NAF-1 siRNA, with or without subsequent starvation. Scale bar represents 10 μm. Cell lysates were analysed by immunoblot. All lanes are derived from the same gel and of the same exposure. Thin white line indicates where lanes have been removed. Autophagy levels observed by electron microscopy (**C**) were quantified and expressed as either the percentage of cells containing autophagic vacuoles (**D**) or the number of autophagosomes per cell (**E**). A minimum of 100 cells per sample were counted; results represent the average ± s.e.m.

immediate rise in cytoplasmic Ca^{2+}, the magnitude of which depends on the ER Ca^{2+} levels. As shown in Figure 6Aa, b and B, NAF-1 knockdown had no effect on the steady-state level or releasable Ca^{2+} from the ER in H1299 cells. However, the otherwise depressed ER Ca^{2+} levels in H1299 cells expressing BCL-2b5 were returned to near normal (control) (Figure 6Ac, d and B). Furthermore, similar to BCL-2b5, endogenous NAF-1 physically associates with endogenous IP3 receptor type 1 as judged by co-immunoprecipitation (Figure 6C). Thus, NAF-1 is linked physically and functionally to the regulation of an important target of BCL-2 at the ER, the IP3 receptor.

Discussion

This study reports the identity of NAF-1, a small (15 kDa), earlier uncharacterized single-spanning integral membrane protein located at the ER, and shows that NAF-1 is a binding

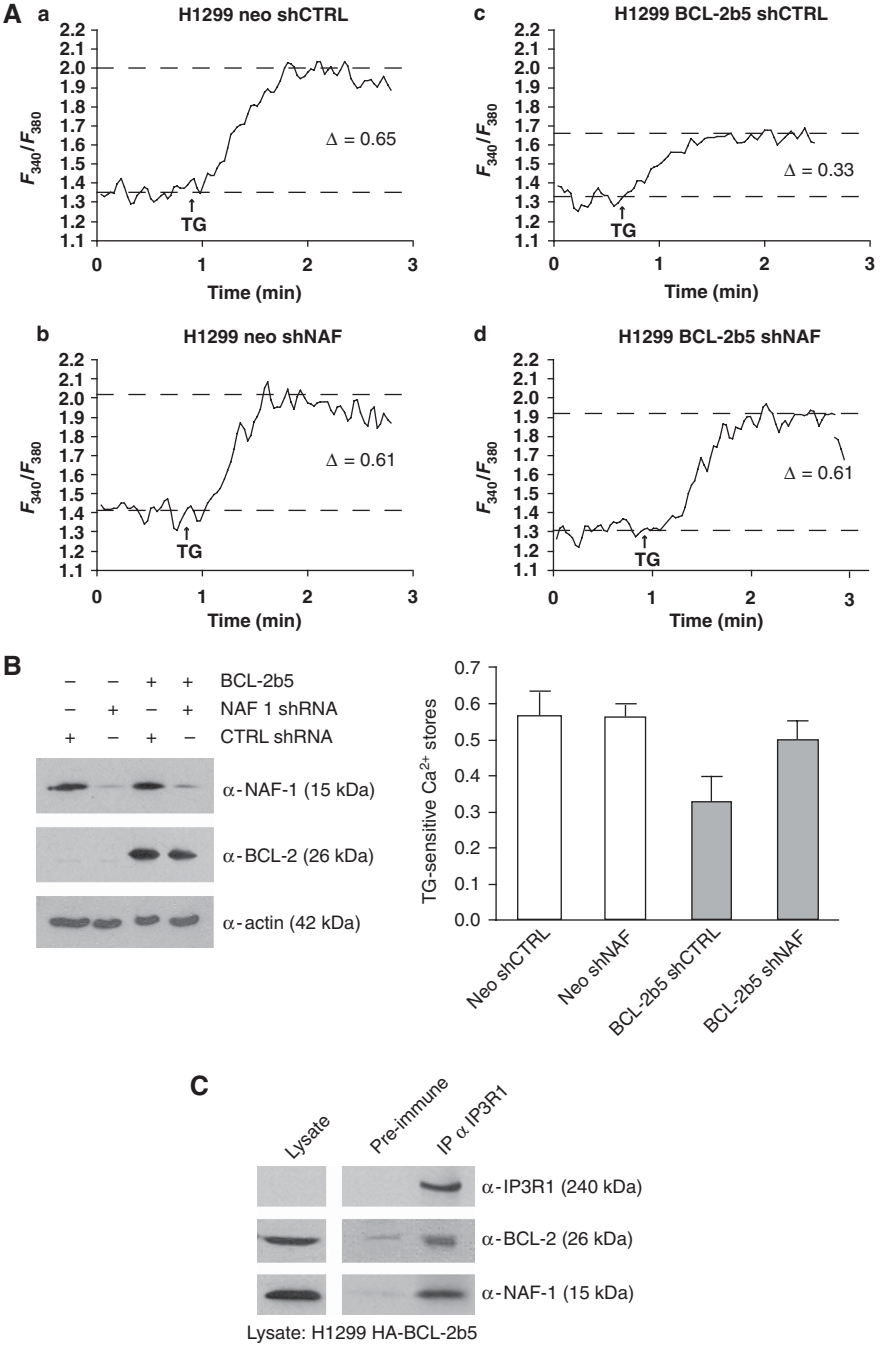

Figure 6 NAF-1 knockdown reverses BCL-2 lowering of ER Ca^{2+} stores. (**A**) H1299 neo and HA-BCL-2b5 cells treated with either CTRL or NAF-1 shRNA were loaded with Fura-2AM, and ER Ca^{2+} stores were measured as the difference in cytoplasmic Ca^{2+} concentration before and after addition of TG (2 μM). Shown are representative traces of Fura-2AM fluorescence measured at 340/380 nm excitation wavelength ratio at 510 nm wavelength emission. Arrow indicates time at which TG was added, delta values indicate TG-sensitive ER Ca^{2+} stores. (**B**) Differences in ER Ca^{2+} stores are shown as the average ± s.e.m. of three independent experiments as described in (**A**). (**C**) Co-immunoprecipitation of endogenous NAF-1 and endogenous IP3 receptor type I. Lysate from H1299 HA-BCL-2b5 cells was collected and immunoprecipitation was performed with anti-IP3R1 antibody. The resulting precipitate was analysed by immunoblot.

partner of BCL-2 at this membrane. Using different methodologies, the results further indicate that NAF-1 seems to be required for BCL-2 at this site to inhibit Beclin 1-mediated autophagy in response to nutrient deprivation in H1299 epithelial cells. Beclin 1 has been identified as a BH3-only protein (Oberstein *et al*, 2007), lending credence to the model that BCL-2 antagonizes Beclin 1-mediated autophagy through direct binding and inhibition of Beclin 1 (Pattingre *et al*, 2005; Maiuri *et al*, 2007). Given that Beclin 1 is a non-membrane protein and has a weak BH3 domain (Feng *et al*, 2007; Oberstein *et al*, 2007), however, the fact that BCL-2 located at the ER can inhibit Beclin 1 requires further elucidation. Recent work, for example, suggests that part of the class III PI3K population that is responsible for generating a PI(3)P-enriched membrane compartment that can nucleate the formation of pre-autophagosomal vesicles, may be assembled at a site associated with the ER (Axe *et al*, 2008). Interestingly, a non-membrane integrated constituent of this site that associates with PI(3)P (double FYVE domain-containing protein 1) can also be delivered to this site when anchored to the ER membrane through a cytochrome b5 membrane anchor, suggesting that this site can be accessed by lateral diffusion within the ER bilayer. Assembly of the PI3K complex containing Vps34, Beclin 1, and accessory proteins that generates the PI(3)P-enriched compartment at the ER likely involves delivery of Vps34-containing vesicles to the vicinity of the ER, where Vps34 presumably interacts with Beclin 1 (Axe *et al*, 2008). Interestingly, knockdown of NAF-1 resulted in an unusual distribution of LC3 in starved cells, including at blebs or filopodia-like structures at the cell periphery (Figure 4B). As LC3 targets PI(3)P-enriched membrane sites during autophagy, this may indicate that loss of NAF-1 influences the normal biogenesis, distribution, or fate of PI(3)P in response to nutrient depletion.

One possibility is that the ER-associated Beclin 1/Vps34 PI3K complex assembly site is also a site that can be accessed by the BCL-2/NAF-1 membrane-integrated complex at the ER, targeting ER BCL-2 to Beclin 1 for functional inhibition of the Beclin 1/Vps34 PI3K complex. In this context, in which BCL-2 expression was targeted to the ER through BCL-2b5, we showed a clear contribution of endogenous NAF-1 to BCL-2b5/Beclin 1 interactions using NAF-1 siRNA (Figure 5A). In contrast, NAF-1 is not required for BCL-2 interaction with BIK, and BIK is able to inhibit the interaction between BCL-2 and NAF-1 (Figure 1E). The simplest explanation for why NAF-1 targets BCL-2 to the BIK autophagy pathway versus the apoptosis pathway, therefore, is that NAF-1 is required for BCL-2 to interact with and antagonize Beclin 1 interactions, but NAF-1 is not required for BIK to interact with BCL-2 and antagonize its anti-apoptotic function.

A current model suggests that BCL-2 constitutively interacts with Beclin 1 and prevents Beclin 1 from initiating autophagy. An autophagic stimulus such as nutrient deprivation, on the other hand, can result in changes to the phosphorylation status of BCL-2 (Wei *et al*, 2008) or Beclin 1 (Zalckvar *et al*, 2009) to inhibit this interaction. Alternatively, Beclin 1/BCL-2 interactions may be disrupted by a competing BH3-only protein in response to the autophagic stimulus (Maiuri *et al*, 2007). In the BCL-2b5-expressing cells used here, Beclin 1 was predominantly distributed throughout the cell as judged by immunofluorescence (data not shown), consistent with the idea that the BCL-2/NAF-1 complex at the ER is targeting a sub-population of Beclin 1. NAF-1 does not contain a BH3 domain, as expected if NAF-1 promotes BCL-2/Beclin 1 interactions (otherwise NAF-1 would compete with Beclin 1 for interaction with BCL-2). BH3-independent interactions between BCL-2 and certain binding partners have earlier been observed, notably the interaction between BCL-2 and the IP3 receptor at the ER (Rong *et al*, 2009). In the case of NAF-1, we identified the CDGSH domain within the cytosolic region as being essential, but not sufficient for NAF-1/BCL-2 interactions. Despite the fact that NAF-1 does not contain a canonical BH3 domain, we also found that the ER-restricted BH3 protein, BIK, was able to displace NAF-1 from BCL-2. Emerging evidence, however, suggests that BCL-2 undergoes significant conformational changes on binding of a potent BH3 ligand (Dlugosz *et al*, 2006; Shore and Nguyen, 2008). Although BIK is not a known physiological stimulus of autophagy and is not induced in response to nutrient deprivation, other more relevant BH3-only proteins such as BAD (Maiuri *et al*, 2007) might interfere with both the Beclin BH3- and the NAF-1-dependent (and potentially other) interactions with BCL-2, disassembling the complex and freeing Beclin 1 from BCL-2 inhibition.

As noted above, the displacement model for Beclin 1 activation assumes that Beclin 1 is constitutively constrained by BCL-2 proteins and is activated on release from the BCL-2 inhibitor. In this model, inhibition of autophagy by elevated BCL-2 presumably arises because the autophagic stimulus cannot overcome the higher BCL-2 sink for Beclin 1. Here, we show that NAF-1 depletion interferes with the ability of BCL-2 to interact with Beclin 1 and strongly overcomes the ability of BCL-2 to inhibit Beclin 1-mediated autophagy in response to nutrient deprivation. Of note, however, and in contrast to the model, depletion of NAF-1 in the absence of a cell starvation stress (i.e. in control cells) does not result in a spontaneous induction of autophagy. This is analogous to the function of BCL-2 in regulating BAX and BAK in response to an apoptotic stimulus (reviewed in Shore and Nguyen, 2008). Knockdown or inhibition of pro-survival BCL-2 proteins leads to cell death only in 'primed' cells (i.e. cells in which sufficient levels of activator BH3-only proteins or some other mechanism are present to activate BAX or BAK once the inhibition by the pro-survival member is removed). In the absence of such a priming mechanism to activate BAX and BAK, then inhibition of pro-survivals does not lead to cell death. Clearly, we show that knockdown of NAF-1 on its own does not activate autophagy in cell lines maintained in 10% serum, but reduces the potential BCL-2/Beclin 1 interaction. In contrast, NAF-1 depletion coupled with nutrient deprivation resulted in enhanced autophagy compared with control cells. This could mean that additional Beclin 1 priming may be required for autophagy induction. It may be, for example, that activation of JNK, which leads to phosphorylation of BCL-2 and disruption of BCL-2/Beclin 1 interactions (Wei *et al*, 2008), or of DAPk, which results in phosphorylation of the Beclin 1 BH3 domain (Zalckvar *et al*, 2009) and disruption of BCL-XL/Beclin 1 interactions, or a number of other stress pathways, results in both the inhibition of BCL-2/Beclin 1 interactions and the activation of parallel 'priming' pathways that activate Beclin 1-mediated autophagy, that is analogous to the regulation of BAX and BAK. Consistent with this model is the finding in mice that, in contrast to nutrient-replete cell culture (this study), targeted deletion of the *wfs2* gene

(*naf-1/cisd2/eris*) resulted in early onset ageing and mortality with evidence of autophagic cell death (Chen *et al*, 2009). Of note, however, this study also reported that embryonic fibroblasts harbouring the *wfs2* gene deletion grew normally in complete medium. One explanation is that the accumulated stress in live animals coupled with loss of NAF-1 expression ultimately leads to enhanced autophagy.

Genetic evidence in Dictyostelium has implicated the IP3 receptor in autophagy (Lam *et al*, 2008) and a recent report has proposed that the receptor may constitute a platform to permit the inhibition of Beclin 1 by BCL-2 (Vicencio *et al*, 2009). In addition, BCL-2-mediated regulation of autophagy through ER Ca^{2+} modulation has been reported (Brady *et al*, 2007; Hoyer-Hansen *et al*, 2007; but see Criollo *et al*, 2007). Given the direct involvement of BCL-2 interaction with the IP3 receptor and regulation of ER Ca^{2+} stores (Heath-Engel *et al*, 2008; Pinton *et al*, 2008), we investigated the influence of NAF-1. Similar to BCL-2b5, endogenous NAF-1 was found in physical association with IP3 receptor type 1. Moreover, elevated BCL-2 at the ER can result in depressed levels of ER Ca^{2+} stores in epithelial cells (Distelhorst and Shore, 2004; Pinton and Rizzuto, 2006), but this property of BCL-2b5 was lost after knockdown of NAF-1 by shRNA. Although further studies are required to determine whether and how the association of the NAF-1/BCL-2 complex with the IP3 receptor regulates autophagy, these findings serve to tie NAF-1 to a major site of BCL-2 regulation at the ER. Furthermore, mitochondrial damage was reported in aged mice harbouring the *wfs2* gene deletion (Chen *et al*, 2009), a fact that can be explained by potential dysregulated Ca^{2+} transmission from the ER to mitochondria through the IP3 receptor.

Finally, the point mutation in the *wfs2* gene results in the theoretical production of a severely truncated version of NAF-1 (Figure 1B), and it is this truncated gene product that represents the underlying aetiology of WFS2, a neurodegenerative condition (Amr *et al*, 2007). As the WFS2 mutation removes a critical BCL-2-binding site within the cytosolic domain of NAF-1, a key question for future studies is the consequences of defective regulation of NAF-1 and presumably autophagy on this and perhaps other degenerative syndromes. Moreover, it will be important to determine whether gene deletion in mice recapitulates the *wfs2* mutation. At least provisionally, ectopic expression of the WFS2 mutant of NAF-1 tagged with HA in H1299 cells, whose endogenous NAF-1 was strongly knocked down by NAF-1 shRNA (which does not target the WFS2 mutant), had no effect on starvation-induced conversion of LC3 (Supplementary Figure 6). Of interest, however, will be the fate of the WFS2 protein and phenotype of transgenic *wfs2*-null mice expressing the WFS2 protein.

Materials and methods

Antibodies

The following antibodies were used in this study: mouse anti-actin (ICN), rabbit anti-Beclin 1 (Santa Cruz), hamster anti-BCL-2 (BD Biosciences), rabbit anti-BCL-XL (Cell Signaling), goat anti-BIK (Santa Cruz), mouse anti-Calnexin (BD Biosciences), rabbit anti-Caspase 3 (Cell Signaling), mouse anti-Cytochrome *c* (BD Biosciences), mouse anti-FLAG M2 (Santa Cruz), mouse anti-GST (Santa Cruz), mouse anti-HA (BAbCO), rabbit anti-IP3R1 (Affinity Bioreagents), rabbit anti-LC3B (Cell Signaling), and rabbit anti-MCL-1 (Stressgen). Rabbit pAbs were raised against the cytosolic domain of NAF-1. Rabbit anti-IP3R1 Rbt03 antibody was kindly provided by Jan Parys (Parys *et al*, 1995).

Cell culture and adenovirus

SK-Mel5, H1299 neo and HA-BCL-2b5 cells were cultured as described earlier (Germain *et al*, 2005; Nguyen *et al*, 2007). To generate H1299 cell lines stably expressing GFP-LC3, cells were transfected with pEGFP-C1 vector (Lipofectamine Plus, Invitrogen) encoding rat LC3 cDNA (gift from Heidi McBride). G418-resistant colonies were screened for expression of GFP-LC3. Adenoviral vectors expressing NAF-1-Flag and NAF-1-mut-Flag were generated and infections were performed as described (Mathai *et al*, 2002). For infections with Ad-BIK, cells were infected for the indicated times and caspase-3 activity assays were conducted as described earlier (Germain *et al*, 2005).

Knockdown of NAF-1 using shRNA and siRNA

For knockdown of NAF-1 with lentiviral shRNA, target sequences were cloned into pSIH1-H1-Puro shRNA Expression Lentivector (System Biosciences). The target sequence for NAF-1 was GGAT AGCTTGATTAATCTT. The non-targeting CTRL shRNA, GATCCAAT AGCGACTAAACACATCAA, was kindly provided by Shengbing Huang (Huang and Sinicrope, 2008). Pseudovirus production and lentivirus infections were carried out using the pPACKH1 Lentivector Packaging kit (System Biosciences) according to manufacturer's protocol. Forty-eight hours after infection with the lentivirus and selection with puromycin, cells were treated as described. siRNA smart pools for NAF-1, Beclin 1, and Luciferase were purchased from Dharmacon. Cells were transfected with 100 nM siRNA using Lipofectamine 2000 (Invitrogen), 24 h post-transfection cells were split and re-transfected with siRNA at 48 h, at 72 h cells were treated or collected as described.

Purification of NAF-1

LM from H1299 BCL-2b5 cells (Germain *et al*, 2002) was cross-linked with 1 mM BMH (Pierce). Cross-linked LM was subjected to preparative 8.5% SDS–PAGE (Ng *et al*, 1997). Fractions containing NAF-1/BCL-2 were combined and 10 × RIPA buffer (0.5 M Tris pH 7.2, 0.45 M NaCl, 10% sodium deoxycholate, 10% Triton X-100) was added to modify the solution for immunoprecipitation. The precipitate was resolved by SDS–PAGE and stained with Colloidal Blue (Invitrogen). The corresponding band was excised and analysed by microcapillary reverse-phase HPLC nano-electrospray tandem mass spectrometry (μLC/MS/MS) on a Finnigan LCQ DECA XP Plus quadrupole ion trap mass spectrometer at the Harvard Microchemistry Facility.

Cloning of NAF-1

NAF-1 cDNA was cloned by RT–PCR using H1299 mRNA and PCR primers derived from the human NAF-1 sequence (GeneBank Accession NM_001008388). The primers used were 5′-CCGGATCC AGGATGGTGCTGGAGAGCGTGGCCCGT-3′ and 5′-CCGAATTCTGTT CAACCAGTAGTAATAATT-3′, containing BamHI and EcoRI sites, respectively. PCR was used to insert a Flag-tag upstream of the KKKEV ER localization signal. To generate the cytosolic domain of NAF-1, the primer 5′-CCGGATCCCTCCCGAAGAAGAAACAACA GAAG-3′ was used with the reverse primer of full-length NAF-1 and cloned into pGEX 2T. The C99S C101S C110S H114Q NAF-1 mutant was generated by PCR site-directed mutagenesis.

Immunofluorescence

H1299 cells were seeded onto glass coverslips and samples were prepared and visualized as described earlier (Germain *et al*, 2005).

Immunoprecipitation

Immunoprecipitation was performed from whole cell extracts or cross-linked LM and then analysed by immunoblot using the antibodies indicated. Immnoprecipitations performed with anti-NAF-1 or anti-BCL-2 antibody were carried out as described earlier (Breckenridge *et al*, 2002). Immunoprecipitation of IP3R1 was performed as described (Chen *et al*, 2004) using anti-IP3R1 Rbt03 antibody.

GST pulldowns

GST-fusion proteins were purified and coupled to glutathione beads using the GST Gene Fusion System (GE Healthcare). HA-BCL-2ΔTM

was translated using the TNT® T7 System (Promega). Lysates were diluted in HIM buffer and incubated with GST-fusion protein beads overnight. Beads were washed, eluted with SDS sample buffer, and analysed by western blot.

Autophagy assays

Cells were either starved for 4 h in EBSS (starvation medium) or maintained in αMEM with 10% FCS (normal media). Where indicated, cells were starved in the presence of either Baf A1 (Sigma) at 100 nM or DMSO vehicle. For immunoblot analysis of LC3 conversion, cells were lysed, resolved by 15% SDS–PAGE, and transferred in CAPS transfer buffer as described (Swerdlow *et al*, 2008). For analysis of GFP-LC3, GFP-LC3 staining of cells was visualized by light microscopy and autophagy was measured by quantitation of the percentage of GFP-LC3-expressing cells displaying punctate GFP-LC3. A minimum of 100 cells per sample was counted for triplicate samples. For analysis by electron microscopy, cells were grown on glass coverslips, fixed, prepared, and examined as described earlier (Germain *et al*, 2005). Autophagy was measured by quantitation of the percentage of counted cells containing autophagic vacuoles and by quantifying the average number of autophagosomes per cell for each sample. A minimum of 100 cells per sample was counted.

ER Ca^{2+} measurements

ER Ca^{2+} stores of H1299 neo and HA-BCL-2b5 cells treated with either CTRL or NAF-1 shRNA were measured as described earlier (Germain *et al*, 2005).

Supplementary data

Supplementary data are available at *The EMBO Journal* Online (http://www.embojournal.org).

Acknowledgements

We thank Heidi McBride, Jan Parys, and Shengbing Huang for providing reagents and suggestions. We are very grateful to Peter Rippstein, Yongjie Wei, Bill Lane, Jean-Paul Decuypere, Nhi Nguyen, and Mary Sutherland for discussions and excellent technical help. NC Chang is a recipient of the Canadian Institutes of Health Research Canada Graduate Scholarships Doctoral award. This work was supported by grants from the Canadian Institutes of Health Research and the Canadian Cancer Society.

Conflict of interest

The authors declare that they have no conflict of interest.

References

Amr S, Heisey C, Zhang M, Xia XJ, Shows KH, Ajlouni K, Pandya A, Satin LS, El-Shanti H, Shiang R (2007) A homozygous mutation in a novel zinc-finger protein, ERIS, is responsible for Wolfram syndrome 2. *Am J Hum Genet* **81:** 673–683

Axe EL, Walker SA, Manifava M, Chandra P, Roderick HL, Habermann A, Griffiths G, Ktistakis NT (2008) Autophagosome formation from membrane compartments enriched in phosphatidylinositol 3-phosphate and dynamically connected to the endoplasmic reticulum. *J Cell Biol* **182:** 685–701

Boyd JM, Gallo GJ, Elangovan B, Houghton AB, Malstrom S, Avery BJ, Ebb RG, Subramanian T, Chittenden T, Lutz RJ, Chinnadurai G (1995) Bik, a novel death-inducing protein shares a distinct sequence motif with Bcl-2 family proteins and interacts with viral and cellular survival-promoting proteins. *Oncogene* **11:** 1921–1928

Brady NR, Hamacher-Brady A, Yuan H, Gottlieb RA (2007) The autophagic response to nutrient deprivation in the hl-1 cardiac myocyte is modulated by Bcl-2 and sarco/endoplasmic reticulum calcium stores. *FEBS J* **274:** 3184–3197

Breckenridge DG, Nguyen M, Kuppig S, Reth M, Shore GC (2002) The procaspase-8 isoform, procaspase-8L, recruited to the BAP31 complex at the endoplasmic reticulum. *Proc Natl Acad Sci USA* **99:** 4331–4336

Chen R, Valencia I, Zhong F, McColl KS, Roderick HL, Bootman MD, Berridge MJ, Conway SJ, Holmes AB, Mignery GA, Velez P, Distelhorst CW (2004) Bcl-2 functionally interacts with inositol 1,4,5-trisphosphate receptors to regulate calcium release from the ER in response to inositol 1,4,5-trisphosphate. *J Cell Biol* **166:** 193–203

Chen YF, Kao CH, Chen YT, Wang CH, Wu CY, Tsai CY, Liu FC, Yang CW, Wei YH, Hsu MT, Tsai SF, Tsai TF (2009) Cisd2 deficiency drives premature aging and causes mitochondria-mediated defects in mice. *Genes Dev* **23:** 1183–1194

Ciechomska IA, Goemans GC, Skepper JN, Tolkovsky AM (2009) Bcl-2 complexed with Beclin-1 maintains full anti-apoptotic function. *Oncogene* **28:** 2128–2141

Criollo A, Maiuri MC, Tasdemir E, Vitale I, Fiebig AA, Andrews D, Molgo J, Diaz J, Lavandero S, Harper F, Pierron G, di Stefano D, Rizzuto R, Szabadkai G, Kroemer G (2007) Regulation of autophagy by the inositol trisphosphate receptor. *Cell Death Differ* **14:** 1029–1039

Distelhorst CW, Shore GC (2004) Bcl-2 and calcium: controversy beneath the surface. *Oncogene* **23:** 2875–2880

Dlugosz PJ, Billen LP, Annis MG, Zhu W, Zhang Z, Lin J, Leber B, Andrews DW (2006) Bcl-2 changes conformation to inhibit Bax oligomerization. *EMBO J* **25:** 2287–2296

Feng W, Huang S, Wu H, Zhang M (2007) Molecular basis of Bcl-xL's target recognition versatility revealed by the structure of Bcl-xL in complex with the BH3 domain of Beclin-1. *J Mol Biol* **372:** 223–235

Germain M, Mathai JP, McBride HM, Shore GC (2005) Endoplasmic reticulum BIK initiates DRP1-regulated remodelling of mitochondrial cristae during apoptosis. *EMBO J* **24:** 1546–1556

Germain M, Mathai JP, Shore GC (2002) BH-3-only BIK functions at the endoplasmic reticulum to stimulate cytochrome c release from mitochondria. *J Biol Chem* **277:** 18053–18060

Heath-Engel HM, Chang NC, Shore GC (2008) The endoplasmic reticulum in apoptosis and autophagy: role of the BCL-2 protein family. *Oncogene* **27:** 6419–6433

Hoyer-Hansen M, Bastholm L, Szyniarowski P, Campanella M, Szabadkai G, Farkas T, Bianchi K, Fehrenbacher N, Elling F, Rizzuto R, Mathiasen IS, Jaattela M (2007) Control of macroautophagy by calcium, calmodulin-dependent kinase kinase-beta, and Bcl-2. *Mol Cell* **25:** 193–205

Huang S, Sinicrope FA (2008) BH3 mimetic ABT-737 potentiates TRAIL-mediated apoptotic signaling by unsequestering Bim and Bak in human pancreatic cancer cells. *Cancer Res* **68:** 2944–2951

Inbal B, Bialik S, Sabanay I, Shani G, Kimchi A (2002) DAP kinase and DRP-1 mediate membrane blebbing and the formation of autophagic vesicles during programmed cell death. *J Cell Biol* **157:** 455–468

Jackson MR, Nilsson T, Peterson PA (1990) Identification of a consensus motif for retention of transmembrane proteins in the endoplasmic reticulum. *EMBO J* **9:** 3153–3162

Kihara A, Kabeya Y, Ohsumi Y, Yoshimori T (2001) Beclin-phosphatidylinositol 3-kinase complex functions at the trans-Golgi network. *EMBO Rep* **2:** 330–335

Lam D, Kosta A, Luciani MF, Golstein P (2008) The inositol 1,4,5-trisphosphate receptor is required to signal autophagic cell death. *Mol Biol Cell* **19:** 691–700

Levine B, Sinha S, Kroemer G (2008) Bcl-2 family members: dual regulators of apoptosis and autophagy. *Autophagy* **4:** 600–606

Liang XH, Jackson S, Seaman M, Brown K, Kempkes B, Hibshoosh H, Levine B (1999) Induction of autophagy and inhibition of tumorigenesis by beclin 1. *Nature* **402:** 672–676

Maiuri MC, Le Toumelin G, Criollo A, Rain JC, Gautier F, Juin P, Tasdemir E, Pierron G, Troulinaki K, Tavernarakis N, Hickman JA, Geneste O, Kroemer G (2007) Functional and physical interaction between Bcl-X(L) and a BH3-like domain in Beclin-1. *EMBO J* **26:** 2527–2539

Mathai JP, Germain M, Marcellus RC, Shore GC (2002) Induction and endoplasmic reticulum location of BIK/NBK in response to apoptotic signaling by E1A and p53. *Oncogene* **21:** 2534–2544

McBride HM, Millar DG, Li JM, Shore GC (1992) A signal-anchor sequence selective for the mitochondrial outer membrane. *J Cell Biol* **119:** 1451–1457

Mizushima N, Yamamoto A, Matsui M, Yoshimori T, Ohsumi Y (2004) *In vivo* analysis of autophagy in response to nutrient starvation using transgenic mice expressing a fluorescent autophagosome marker. *Mol Biol Cell* **15:** 1101–1111

Mizushima N, Yoshimori T (2007) How to interpret LC3 immunoblotting. *Autophagy* **3:** 542–545

Ng FW, Nguyen M, Kwan T, Branton PE, Nicholson DW, Cromlish JA, Shore GC (1997) p28 Bap31, a Bcl-2/Bcl-XL- and procaspase-8-associated protein in the endoplasmic reticulum. *J Cell Biol* **139:** 327–338

Nguyen M, Marcellus RC, Roulston A, Watson M, Serfass L, Murthy Madiraju SR, Goulet D, Viallet J, Belec L, Billot X, Acoca S, Purisima E, Wiegmans A, Cluse L, Johnstone RW, Beauparlant P, Shore GC (2007) Small molecule obatoclax (GX15-070) antagonizes MCL-1 and overcomes MCL-1-mediated resistance to apoptosis. *Proc Natl Acad Sci USA* **104:** 19512–19517

Oakes SA, Scorrano L, Opferman JT, Bassik MC, Nishino M, Pozzan T, Korsmeyer SJ (2005) Proapoptotic BAX and BAK regulate the type 1 inositol trisphosphate receptor and calcium leak from the endoplasmic reticulum. *Proc Natl Acad Sci USA* **102:** 105–110

Oberstein A, Jeffrey PD, Shi Y (2007) Crystal structure of the Bcl-XL-Beclin 1 peptide complex: Beclin 1 is a novel BH3-only protein. *J Biol Chem* **282:** 13123–13132

Parys JB, de Smedt H, Missiaen L, Bootman MD, Sienaert I, Casteels R (1995) Rat basophilic leukemia cells as model system for inositol 1,4,5-trisphosphate receptor IV, a receptor of the type II family: functional comparison and immunological detection. *Cell Calcium* **17:** 239–249

Pattingre S, Tassa A, Qu X, Garuti R, Liang XH, Mizushima N, Packer M, Schneider MD, Levine B (2005) Bcl-2 antiapoptotic proteins inhibit Beclin 1-dependent autophagy. *Cell* **122:** 927–939

Pinton P, Giorgi C, Siviero R, Zecchini E, Rizzuto R (2008) Calcium and apoptosis: ER-mitochondria Ca2 + transfer in the control of apoptosis. *Oncogene* **27:** 6407–6418

Pinton P, Rizzuto R (2006) Bcl-2 and Ca2 + homeostasis in the endoplasmic reticulum. *Cell Death Differ* **13:** 1409–1418

Rashmi R, Pillai SG, Vijayalingam S, Ryerse J, Chinnadurai G (2008) BH3-only protein BIK induces caspase-independent cell death with autophagic features in Bcl-2 null cells. *Oncogene* **27:** 1366–1375

Rong YP, Barr P, Yee VC, Distelhorst CW (2009) Targeting Bcl-2 based on the interaction of its BH4 domain with the inositol 1,4,5-trisphosphate receptor. *Biochim Biophys Acta* **1793:** 971–978

Shore GC, Nguyen M (2008) Bcl-2 proteins and apoptosis: choose your partner. *Cell* **135:** 1004–1006

Simpson JC, Wellenreuther R, Poustka A, Pepperkok R, Wiemann S (2000) Systematic subcellular localization of novel proteins identified by large-scale cDNA sequencing. *EMBO Rep* **1:** 287–292

Swerdlow S, McColl K, Rong Y, Lam M, Gupta A, Distelhorst CW (2008) Apoptosis inhibition by Bcl-2 gives way to autophagy in glucocorticoid-treated lymphocytes. *Autophagy* **4:** 612–620

Vicencio JM, Ortiz C, Criollo A, Jones AW, Kepp O, Galluzzi L, Joza N, Vitale I, Morselli E, Tailler M, Castedo M, Maiuri MC, Molgo J, Szabadkai G, Lavandero S, Kroemer G (2009) The inositol 1,4,5-trisphosphate receptor regulates autophagy through its interaction with Beclin 1. *Cell Death Differ* **16:** 1006–1017

Wang B, Heath-Engel H, Zhang D, Nguyen N, Thomas DY, Hanrahan JW, Shore GC (2008) BAP31 interacts with Sec61 translocons and promotes retrotranslocation of CFTRDeltaF508 via the derlin-1 complex. *Cell* **133:** 1080–1092

Wei Y, Pattingre S, Sinha S, Bassik M, Levine B (2008) JNK1-mediated phosphorylation of Bcl-2 regulates starvation-induced autophagy. *Mol Cell* **30:** 678–688

White C, Li C, Yang J, Petrenko NB, Madesh M, Thompson CB, Foskett JK (2005) The endoplasmic reticulum gateway to apoptosis by Bcl-X(L) modulation of the InsP3R. *Nat Cell Biol* **7:** 1021–1028

Wiley SE, Murphy AN, Ross SA, van der Geer P, Dixon JE (2007a) MitoNEET is an iron-containing outer mitochondrial membrane protein that regulates oxidative capacity. *Proc Natl Acad Sci USA* **104:** 5318–5323

Wiley SE, Paddock ML, Abresch EC, Gross L, van der Geer P, Nechushtai R, Murphy AN, Jennings PA, Dixon JE (2007b) The outer mitochondrial membrane protein mitoNEET contains a novel redox-active 2Fe-2S cluster. *J Biol Chem* **282:** 23745–23749

Yorimitsu T, Klionsky DJ (2005) Autophagy: molecular machinery for self-eating. *Cell Death Differ* **12**(Suppl 2)**:** 1542–1552

Zalckvar E, Berissi H, Mizrachy L, Idelchuk Y, Koren I, Eisenstein M, Sabanay H, Pinkas-Kramarski R, Kimchi A (2009) DAP-kinase-mediated phosphorylation on the BH3 domain of beclin 1 promotes dissociation of beclin 1 from Bcl-XL and induction of autophagy. *EMBO Rep* **10:** 285–292

Zhu W, Cowie A, Wasfy GW, Penn LZ, Leber B, Andrews DW (1996) Bcl-2 mutants with restricted subcellular location reveal spatially distinct pathways for apoptosis in different cell types. *EMBO J* **15:** 4130–4141

